Spatiotemporal Dynamics of Nitrogen Transport in the Qiandao Lake Basin, a Large Hilly Monsoon Basin of Southeastern China

Dongqiang Chen [1,2], Hengpeng Li [2,*], Wangshou Zhang [2] **, Steven G. Pueppke [3,4]** , **Jiaping Pang [2] and Yaqin Diao [1,2]**

1   University of Chinese Academy of Sciences, Beijing 100049, China; dqchen@niglas.ac.cn (D.C.); yqdiao@niglas.ac.cn (Y.D.)
2   Key Laboratory of Watershed Geographic Sciences, Nanjing Institute of Geography and Limnology, Chinese Academy of Sciences, Nanjing 210008, China; wszhang@niglas.ac.cn (W.Z.); pangjp@niglas.ac.cn (J.P.)
3   Center for Global Change and Earth Observations, Michigan State University, 1405 South Harrison Road, East Lansing, MI 48823, USA; pueppke@msu.edu
4   Asia Hub, Nanjing Agricultural University, Nanjing 210095, China
*   Correspondence: hpli@niglas.ac.cn; Tel.: +86-025-87714759

Abstract: The Qiandao Lake Basin (QLB), which occupies low hilly terrain in the monsoon region of southeastern China, is facing serious environmental challenges due to human activities and climate change. Here, we investigated source attribution, transport processes, and the spatiotemporal dynamics of nitrogen (N) movement in the QLB using the Soil and Water Assessment Tool (SWAT), a physical-based model. The goal was to generate key localized vegetative parameters and agronomic variables to serve as credible information on N sources and as a reference for basin management. The simulation indicated that the basin's annual average total nitrogen (TN) load between 2007 and 2016 was 11,474 tons. Steep slopes with low vegetation coverage significantly influenced the spatiotemporal distribution of N and its transport process. Monthly average TN loads peaked in June due to intensive fertilization of tea plantations and other agricultural areas and then dropped rapidly in July. Subsurface flow is the key transport pathway, with approximately 70% of N loads originating within Anhui Province, which occupies just 58% of the basin area. The TN yields of sub-basins vary considerably and have strong spatial effects on incremental loads entering the basin' major stream, the Xin'anjiang River. The largest contributor to N loads was domestic sewage (21.8%), followed by livestock production (20.8%), cropland (18.6%), tea land (15.5%), forest land (10.9%), atmospheric deposition (5.6%), orchards (4.6%), industry (1.4%), and other land (0.8%). Our simulation underscores the urgency of increasing the efficiency of the wastewater treatment, conserving slope land, and optimizing agricultural management as components of a comprehensive policy to control N pollution in the basin.

Keywords: N sources; spatiotemporal patterns of pollution; N transport processes; Qiandao Lake Basin; fertilization

---

1. Introduction

The nitrogen (N) cycle is dynamic and strongly influenced by both human activities and physical conditions, especially in environmentally sensitive areas that are prone to nutrient pollution [1,2]. Agricultural practices and domestic sewage account for a substantial proportion of released N, which subsequently enters waterways via pathways that are diverse and poorly understood. Climatic

features and geomorphological factors, including intense rainfall, steep slopes, and the presence of easily erodible soils, exacerbate N emission, transport, and export, adding complexity to the problem of pollution control [1–3]. Against this backdrop, access to comprehensive information about spatiotemporal patterns of N distribution becomes a primary concern for pollution management.

Physical-based models are powerful tools to provide detailed information about the key driving factors of N release and transport. Available models include the Hydrological Simulation Program—FORTRAN [4], the Spatially Referenced Regressions On Basin Attributes model [5], the Regional Nutrient Management model [6], the Annualized Agricultural Nonpoint Source model [7], and the Soil and Water Assessment Tool (SWAT) [8]. As confirmed by many studies, SWAT has performed particularly well for nutrient source analysis and the interpretation of transport processes in spatially heterogeneous areas of China [9,10] and elsewhere where agriculture predominates [11,12]. Moreover, SWAT can comprehensively estimate the attribution patterns of nutrients from various diffuse pollution sources [13,14]. Previous applications of SWAT have mainly focused on basins in semi-humid or semiarid zones [15,16], flat regions [17,18], cropland-dominated areas [19,20], and other environments [21]. Much less is known about the ability of this model to provide information on runoff and nutrient cycles in hilly monsoon areas characterized by diverse land use types and the absence of systematic information needed for science-based policy making [2,22].

We address these issues here by employing SWAT to precisely simulate N loads in one of the largest basins of southeastern China, the Qiandao Lake Basin (QLB). This basin, which lies in a typical low hilly area, experiences a monsoon climate and is a critical source of drinking water for Hangzhou, a prefecture-level city with 10 million residents. Total nitrogen (TN) concentration at the basin's outlet increased from approximately 0.75 to 1.12 mg/L during the past 15 years and now exceeds the target concentration (< 1.0 mg/L) for use as a drinking water source [23,24]. Elevated levels of TN have been attributed to socio-economic development, increasing environmental pressure from rapid expansion of tea plantations, and domestic sewage discharge, all of which have adversely affected water quality in this region over the past decade [22,25–27]. Agriculture is especially important, because fertilizer application rates in the basin, which average 436 kg/ha, are excessive compared to the rest of the world—triple those in the United States and double those in Europe and Japan [28]. Moreover, intensive application of fertilizer occurs from March to May, just before the onset of the rainy season, when erosion is most likely [29,30].

In this study, we applied the SWAT model to the QLB to (i) simulate, estimate, and analyze key localized TN parameters including factors influencing loads, source appointment, and spatiotemporal dynamics, (ii) determine how TN delivery and transport are influenced by complex terrain and monsoon climate, and, (iii) inform a more efficient and targeted strategy for controlling nutrient pollution based on a comprehensive understanding of attribution and spatiotemporal patterns of TN.

2. Materials and Methods

2.1. Study Area

The QLB (29°11′ N–30°02′ N, 118°21′ E–119°20′ E) is centered on Qiandao Lake, which was impounded by a hydroelectric dam constructed in the late 1950s [31]. The basin covers an area of 10,369 km^2, of which 4341 km^2 is in Zhejiang Province and 6028 km^2 is in Anhui Province (Figure 1). The main land use types in the basin are forest land (79.4%), followed by orchards (1.4%), cropland (8.2%), tea land (3.8%), water body (5.4%), and other land (1.8%). The annual average precipitation within the Zhejiang and Anhui portions of the basin is 1498 mm and 1712 mm, respectively. The Xin'anjiang River is the longest and most significant river pathway of the basin. It flows in an eastwardly direction, crossing from Anhui Province to Zhejiang province at Jiekou (location 243.7 km, Figure 1), and proceeding to the basin's outlet at Baqian (location 320.4 km, Figure 1), which lies just above the dam. The middle and lower reaches of the river below Baqian are known locally as the Fuchun River and the Qiantang River; ultimately, the water empties into the East China Sea.
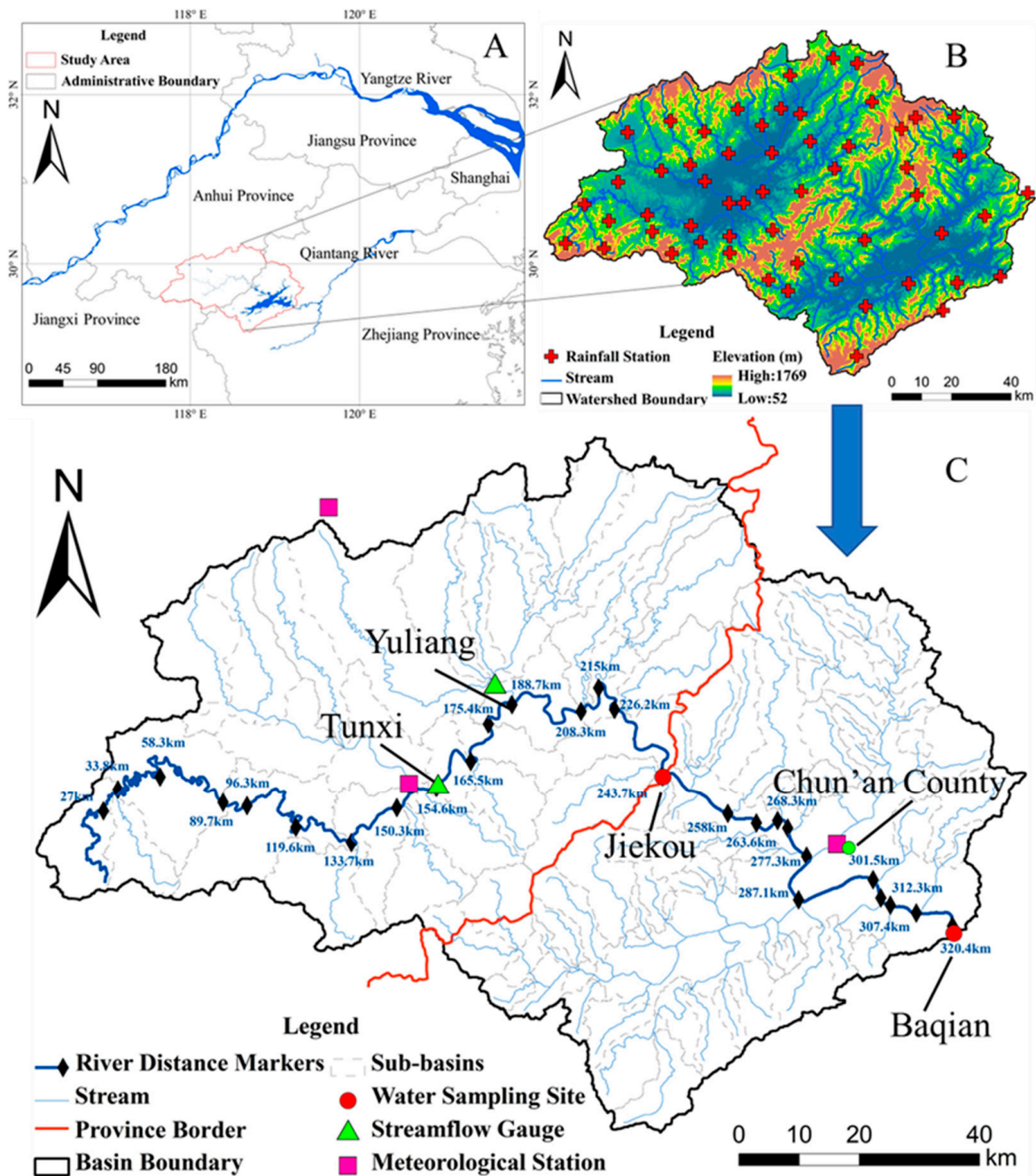
Figure 1. The Qiandao Lake Basin (QLB). (**A**) The Yangtze River delta region showing the orientation of the basin in Anhui and Zhejiang provinces. (**B**) Topography of the basin showing elevations and the location of rainfall stations. (**C**) Detailed map of the basin showing streams, sub-basins, important monitoring sites, and distance markers along the reach of the Xin'anjiang River. The location of the urban core of Chun'an County is also given.

2.2. Data Collection

As shown in Figure 1, the entire QLB was delineated into 96 sub-basins based on the 25-meter digital elevation model. High resolution, 2.1-meter land use data were derived from ZY-3 satellite imagery for 2015, which was purchased from the Chinese Geographical Monitoring Cloud Platform (http://www.dsac.cn/Data/Product/Detail/1009). Whenever possible, e.g., for forest land and built land, default parameters from the land use database were used in SWAT. eCognition Developer, an

object-based tool for automatic analysis of remotely sensed data (http://www.ecognition.com/suite/ecognition-developer), was employed to identify land use types that are typical for the area, e.g., tea land and orchard land. Multiresolution segmentation was adopted for this purpose, with scope of classification algorithms from sample-based nearest neighbor analysis. Every imagery object was checked by visual interpretation, with verification by field observations at 100 separate sites in the basin. The final land use classification map is shown in Figure S1 (see Supplementary Materials for Figure S1).

Soil types and their physical properties were extracted from databases of the Nanjing Institute of Soil Science and, when necessary, verified by field sampling to generate the map shown in Figure S2 (see Supplementary Materials for Figure S2). Distributed rainfall data were collected from 54 rainfall gauges within the QLB (Figure 1). Daily streamflow data from two hydrological stations (Tunxi and Yuliang, see Figure 1) were obtained from the Huangshan Hydrology Bureau and published in Chinese Hydrological Yearbooks [32]. Monthly water quality data were from records of the Chun'an Environmental Protection Bureau. TN data, expressed as the sum of different forms of nitrogen including ammonia, nitrate, nitrite and organic N, were measured according to the National Surface Water Quality Standard (GB 3838-2002) and obtained from the Chun'an Environmental Protection Bureau, which also supplied precipitation and dry deposition data used to determine atmospheric deposition of TN.

The Chun'an Environmental Protection Bureau and Chun'an County Statistical Yearbooks [33,34] provided additional information for the model, including the locations of industrial and domestic wastewater outlets and discharge from them. The spatial distribution of livestock production facilities, their scales of production, and discharge from them was based on governmental monitoring of wastewater streams. Supplemental Information about cropping systems, agronomic practices, management decisions, and rural sewage treatment was obtained from detailed governmental interviews with 487 farmers from 44 villages in the study region. Sewage in the QLB is collected into centralized treatment facilities that discharge wastewater into nearby rivers, and thus for the purpose of SWAT modeling, domestic, industrial, and animal agricultural pollution sources could be generalized as point sources that discharge into point outlets.

2.3. SWAT Model Configuration

Soil data (Figure S2) were transformed into a modeling format by means of standardized definition and interpretation of SWAT parameters, and discharge and associated TN loads from domestic, industrial, and animal agriculture from each sub-basin were configured into the model as described above. Source attribution of atmospheric N deposition was generalized as the single direct source of pollution into water bodies as follows: deposition of ammonium (0.97 mg/L), deposition of nitrate (0.73 mg/L), dry deposition of ammonium (0.434 kg/ha/yr), and dry deposition of nitrate (0.61 kg/ha/yr).

Information from field surveys of agricultural practices in the QLB was used to guide the scheduling of cropland, tea land, and orchard management for the model. Cropland and orchards were operated with heat unit scheduling, but because of its unique growth and management characteristics, tea land was operated with date scheduling in Table S1 (see Supplementary Materials for Table S1). Localized parameters for tea land were optimized on the basis of multi-year field measurements during the growth season, as well as information obtained in similar areas of southeastern China, and then manually assembled into the final input suite for the SWAT database (Table S1).

The previously used SUFI-2 algorithm was employed to analyze the sensitivity, calibration, validation, and uncertainty of the SWAT model [35,36]. Three statistical indicators were utilized to evaluate the model's performance during calibration and validation: the coefficient of determination (R^2), which is an indicator of the goodness of fit between the observed and simulated results; the Nash–Sutcliffe simulation efficiency (ENS), which determines the ability of the model to predict the 1:1 line of correspondence between the observed and simulated values; and PBIAS (Percent bias), which measures the average tendency of simulated values to be larger or smaller than corresponding

observed values [37,38]. Previously defined metrics of model performance were adopted. These assign satisfactory, good, and very good performance to ENS values of 0.5, 0.65, and 0.75, and R^2 values of 0.6, 0.7, and 0.8, respectively [39,40]. PBIAS values of ±25% and ±25% ≤ ±40% are considered to indicate very good and good model performance for N, respectively. The corresponding values for streamflow are ±10% and ±10% ≤ ±15%, respectively.

The SWAT model was used for simulations during the interval from 2003 to 2016. The first four-year interval, from 2003 to 2006, was employed as a warm-up period to allow the streamflow variables to reach a limited range of initial values (see Table S2 for details in Supplementary Materials). Observed daily data from 2007 to 2012 were subsequently used for calibration and those from 2013 to 2016 for validation. N load simulations at the two sampling sites, e.g., Jiekou and Baqian, were executed simultaneously, and iterations of the entire model were performed until satisfactory results were obtained.

3. Results

3.1. Calibration and Sensitivity Analysis of the SWAT Model

Parameters such as cropping systems, fertilization protocols, and soil conditions can vary significantly in different basins, with substantial impacts on modeling outcomes [15,18,41]. Appropriate calibration with parameters that are optimized for the QLB is consequently important, especially for tea, which is intensively managed, known to have undergone considerable expansion during the study period, and recognized to be an important source of nutrient pollution [42,43]. Twenty-one optimized SWAT parameters for tea land in the QLB are given in Table S2. Three crucial parameters (Table 1) diverge significantly from those provided by the SWAT model for forest land and land used for cultivation of other crops. This indicates that both maximum root depth and harvest index are comparatively low for tea, but demand for N in seed is relatively high.

Table 1. Comparison of key Soil and Water Assessment Tool (SWAT) parameter values derived for tea with those available for other crops grown in the QLB.

Parameter	Definition	Cropland	Orchard	Forest Land	Tea Land
HVSTI	Harvest index for land cover/plant [(kg/ha)/kg/ha)]	0.45	0.10	0.76	0.07
RDMX	Maximum root depth for land cover/plant (m)	2.0	2.0	3.5	0.5
CNYLD	Normal fraction of nitrogen in seed for land cover/plant (kg N/kg seed)	0.0199	0.0019	0.0015	0.0246

The most important and sensitive parameters during the calibration of the SWAT model were groundwater (.gw), soil (.sol), basins (.bsn), and management (.mgt). In agreement with previous studies, the moisture condition II curve of the soil conservation service (SCS) curve number method (CN2) was the most sensitive parameter for streamflow [18,36]. This was also the key parameter for runoff yield, as would be expected in a basin characterized by a hilly terrain, agricultural land, and abundant rainfall. Other important parameters representing land-cover features were OV_N, CANMX, HRU_SLP, GWQMN, SOL_AWC, TRNSRCH, and ALPHA_BNK. The most sensitive parameters during calibration of TN loads included N source, transport process, and transformation. The most sensitive nitrogen source parameters were RCN, CMN, SOL_NO3, and FRT_SURFACE, and the most sensitive N transformation and transport process parameters were NPERCO, LAT_ORGN, ERORGN, and BIOMIX.

Overall attribution patterns of TN pollution sources are quite variable across the QLB (Table 2). CN2, a function of land use and soil permeability and thus runoff yield, was the most sensitive hydrological parameter for streamflow and TN output in the basin. Low calibrated values for the initial nitrate concentration in the soil layer and for the N percolation coefficient provide evidence that lateral flow in the shallow soil layer covering much of the basin's steep topography is the main pathway of TN loads. These observations are consistent with an earlier SWAT modeling effort that was confined to the upper half of the basin in Anhui Province [44]. However, a small Manning's 'n' value and low transmission losses (Table 2) indicate that, in contrast to findings of the earlier study, surface and lateral runoff significantly affect TN transport and loss across the basin. We attribute these differences to the larger, basin-wide scope of the current study area, which alters fundamental topographic (Figure 1) and land use (Figure S1) relationships and includes soil types not prevalent in the upper basin (Figure S2).

Table 2. Key parameter values and sensitivities for streamflow and total nitrogen (TN) load simulation in the QLB.

Parameter	Definition	Range	Calibrated Value
Hydrology			
CN2.mgt (Forest land)	Default SCS curve number for moisture conditions	35–98	97.9261
OV_N.hru	Default Manning's 'n' value for overland flow	0.01–30	0.9790
TRNSRCH.bsn	Fraction of transmission losses partitioned to the deep aquifer	0–1	0.0039
Nitrogen			
RCN.bsn	Concentration of nitrogen in rainfall	0–15	0.0412
NPERCO.bsn	Nitrogen percolation coefficient	0–1	0.0020
SOL_NO3.chm	Initial nitrate conc. in soil layer	0–100	27.5619

3.2. Validation of Streamflow and TN Loads

Distributed rainfall data, which are critical for understanding spatiotemporal dimensions of key nutrient transport processes in hilly areas [45,46], exhibited strong annual variation, ranging from a low of 1375 mm to a high of 2373 mm (see Figure S3 in Supplementary Materials). Significant annual fluctuation with a coefficient of variation above 0.1 was recorded for the entire basin, and monthly precipitation was, as expected, characterized by spatial heterogeneity [47]. Rainfall tended to rise rapidly from May to June and decrease sharply from June to July. Average monthly rainfall peaked in June (389 mm), which accounted for over 20% of the total annual accumulation (Figure S3).

Rainfall regulates streamflow and TN transport in the QLB, but other driving forces also occur, and monitoring data are limited. Instead of simply relying on the coupling model [12,48], we applied stepwise calibration and validation to the stimulation to optimize model performance in different regions of the basin. TN data are available from the border between the two provinces at Jiekou and from the basin's outlet at Baqian; streamflow data are also available at Baqian and additionally from two upstream stations at Tunxi and Yuliang (Figure 1). Following the warm-up period, the SWAT model was consequently calibrated and validated for the variables available at each of these sites over a decade-long interval from 2007 to 2016 (Figures 2 and 3).
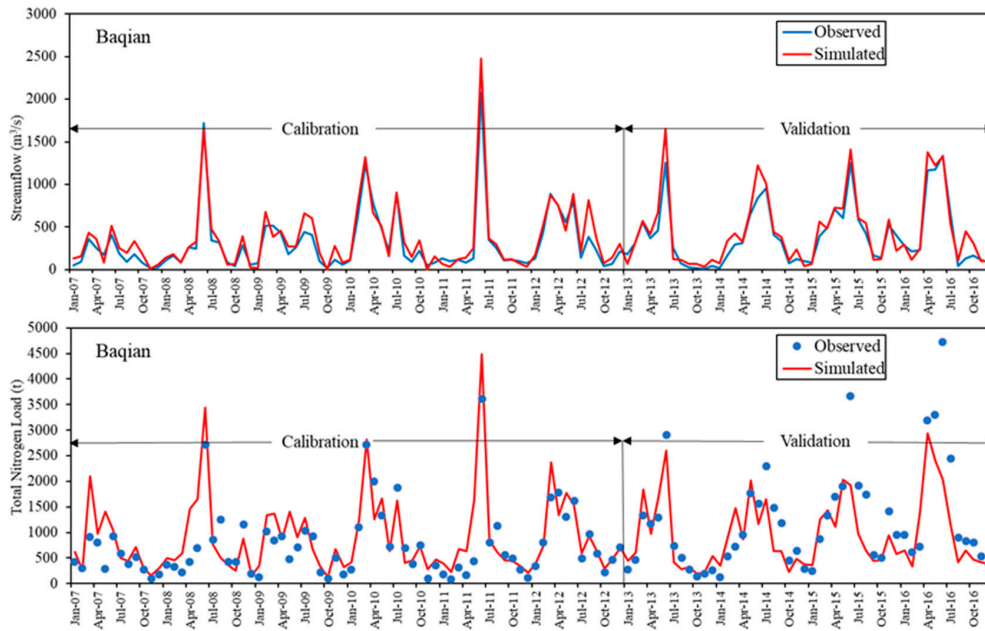
Figure 2. Observed and simulated daily streamflow values and monthly TN loads at the basin's outlet at Baqian.
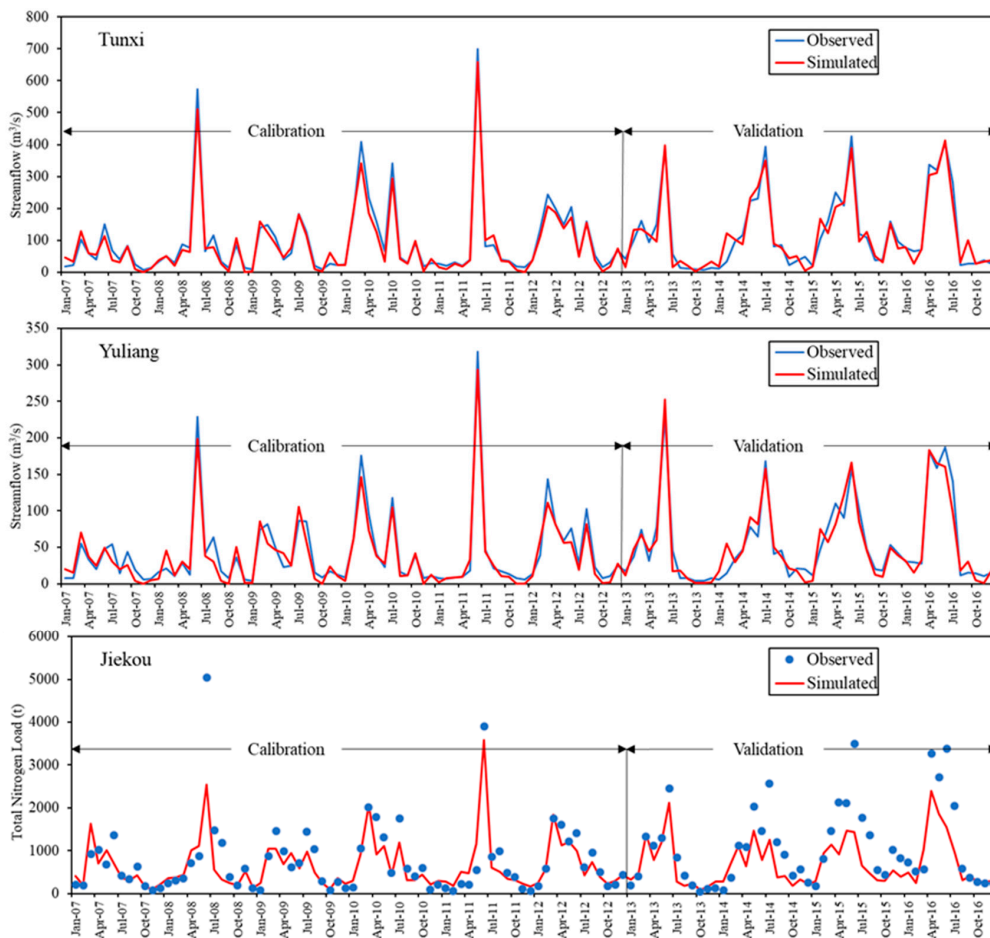
Figure 3. Observed and simulated daily streamflow values at Tunxi and Yuliang, and observed and simulated monthly TN loads at Jiekou.

The correspondence between measured and simulated values for TN and streamflow at Baqian is illustrated in Figure 2. Both variables are characterized by cyclical fluctuations, with annual maxima during the summer rainy season. The TN peaks tend to be displaced to the right compared to corresponding peaks for streamflow, likely because of differences in the frequency of measurement (monthly for TN, daily for streamflow). There is some divergence between observed and simulated TN levels during the peak flow periods of 2015 and 2016, both of which were wet years with extreme rainfall events. R^2 and NSE values (Table 3) are nevertheless indicative of the SWAT model's good and very good performance, respectively, during the calibration and validation periods [35,36].

Table 3. Performance of the SWAT model in simulating streamflow and TN loads in the QLB.

	Station	Streamflow		Station	Total Nitrogen	
		Calibration	Validation		Calibration	Validation
R^2	Baqian	0.97	0.97	Baqian	0.77	0.78
ENS		0.92	0.91		0.65	0.68
PBIAS		−14.4%	−12%		−18.1%	1.3%
R^2	Yuliang	0.95	0.95	Jiekou	0.75	0.71
	Tunxi	0.98	0.97			
ENS	Yuliang	0.94	0.92	Jiekou	0.74	0.62
	Tunxi	0.97	0.93			
PBIAS	Yuliang	9.9%	2.1%	Jiekou	14.6%	22.6%
	Tunxi	8.9%	1.5%			

The SWAT model was also calibrated and validated at sites above the lake and distant from the outlet at Baqian. Observed monthly streamflow at Tunxi and Yuliang was much lower than that at the basin's outlet, and the model accurately simulated this parameter (Figure 3), i.e., the performance of the simulation model at Tunxi and Yuliang was rated as very good according to all three statistical measurements (Table 3). In comparison, performance for streamflow at Baqian was rated as very good by the R^2 and NSE statistics and good by the PBIAS statistic. The model was somewhat less accurate in simulating TN levels at Baqian and Jiekou, especially during the validation period, when TN levels tended to be underestimated (Figure 3). Nevertheless, with just one exception (the NSE statistic at Jiekou during the validation period), model performance at these two sites was uniformly rated as good to very good, indicating that overall model performance was satisfactory.

3.3. Spatiotemporal Patterns of TN Loads and Yields

TN loads over the interval from 2007 to 2016 at the outlet of the QLB are strongly correlated with variations in average rainfall in the basin, both when measured annually (Figure 4A) and monthly (Figure 4B). This indicates that rainfall trends are key drivers of N discharge. TN loads spiked early in the annual fertilization cycle, which begins in March, and reached a maximum in June, when precipitation was also greatest and the risk of erosion highest. Precipitation and TN loads declined thereafter.

The mean annual TN load of the basin was 11,474 t, as calculated from simulations spanning the period 2007–2016. This corresponds to an overall mean TN yield of 1.1 t/km²/yr. The TN point sources that were generalized into three categories for simulation with the SWAT model jointly accounted for 44% of the annual TN load in the basin. The contribution of industrial sources was negligible in comparison to that of domestic sewage and livestock production, which accounted for nearly equivalent amounts of TN loads to the basin (Figure 5A). In addition, nearly 6% of the total could be attributed to atmospheric deposition, with other non-point sources of TN accounting for the remaining half of TN loads in the basin. On a percentage basis, the most important of these sources were cropland and tea land, followed by forest land and orchard land (Figure 5A). These relationships obscure the fact that intensively fertilized tea land contributes 30 times as much TN as forest land does when expressed

in terms of annual TN yields per km² (Figure 5B). Other agricultural land, including orchards and, to a lesser extent, cropland, also account for disproportionate amounts of non-point source TN pollution when measured this way.
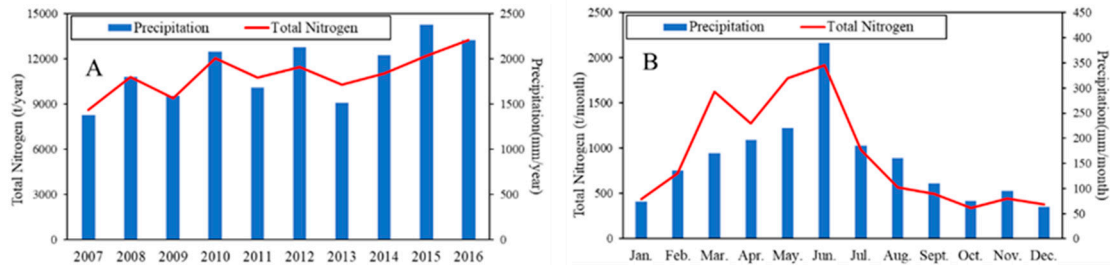
Figure 4. Annual (**A**) and monthly (**B**) variations in precipitation and TN output from the QLB during the interval from 2007 to 2016. Precipitation values were averaged from measurements at 54 sites across the basin, and TN output was measured at the basin's outlet at Baqian.
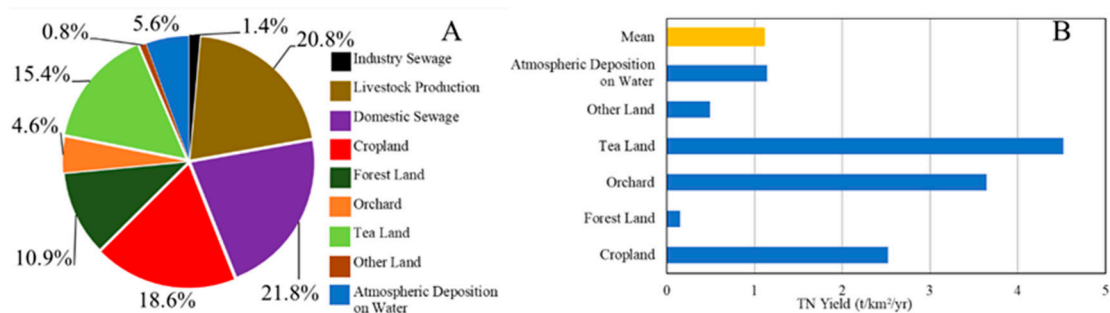
Figure 5. (**A**) Simulated annual contributions of point and non-point sources of pollution to TN loads, as expressed as percentages of the total. (**B**) Simulated annual contributions of non-point sources of pollution, expressed on a per unit area basis, i.e., as TN yields. The yellow bar gives the mean for all land use types.

The spatial patterns of TN loads and TN yields in each of the 96 sub-basins of the QLB are mapped in Figure 6. Upstream sub-basins in Anhui Province jointly account for 70% of the basin's TN loads, but significant sub-basin to sub-basin heterogeneity is obvious, and several hotspots are apparent (Figure 6A). The largest of these lies near the Huangshan City urban core. Downstream riparian areas near the lake also emit significant TN loads, but most sub-basins in Zhejiang Province are relatively minor contributors (Figure 6A). A different pattern emerges when TN yield is considered (Figure 6B). The highest such yields are from a single cluster of sub-basins, and their magnitude tends to progressively diminish with distance from this hotspot. TN yields in other sub-basins, including those near the lake, are generally low. A few additional areas of high TN yield are nevertheless evident, including one near the rapidly urbanizing tourist area in Zhejiang Province's Chun'an County.
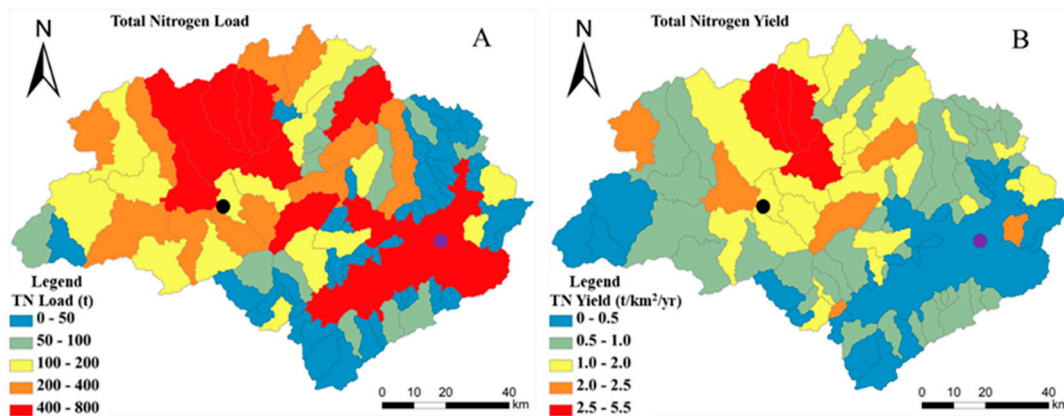
Figure 6. Spatial distribution of annual (**A**) TN loads and (**B**) TN yields among the sub-basins of the QLB. The locations of the urban core of Huangshan City (black dots) and Chun'an County (purple dots) are indicated.

3.4. Sources and Spatial Dynamics of TN Entering the Main Reach of the Xin'anjiang River

Optimization of pollution management requires as much spatiotemporal understanding as possible about sources and transport of pollutants. We consequently used detailed information about TN loads and yields in the sub-basins of the QLB to simulate sources, transport, and entry points of TN pollution into the main stem of the Xin'anjiang River. Figure 7 relates average annual contributions of different pollution sources of TN to their entry along the river's pathway through the QLB. Almost no TN enters the upper 45% of the river's course, but thereafter, three distinct surges of TN become evident. The first, which accounts for 25% of the total TN pollution entering the river (Figure 7), is at Tunxi (location 154.6 km; see Figure 1). Increased discharges of TN from agriculture, especially livestock production, predominate at this site and account for the majority of the surge.
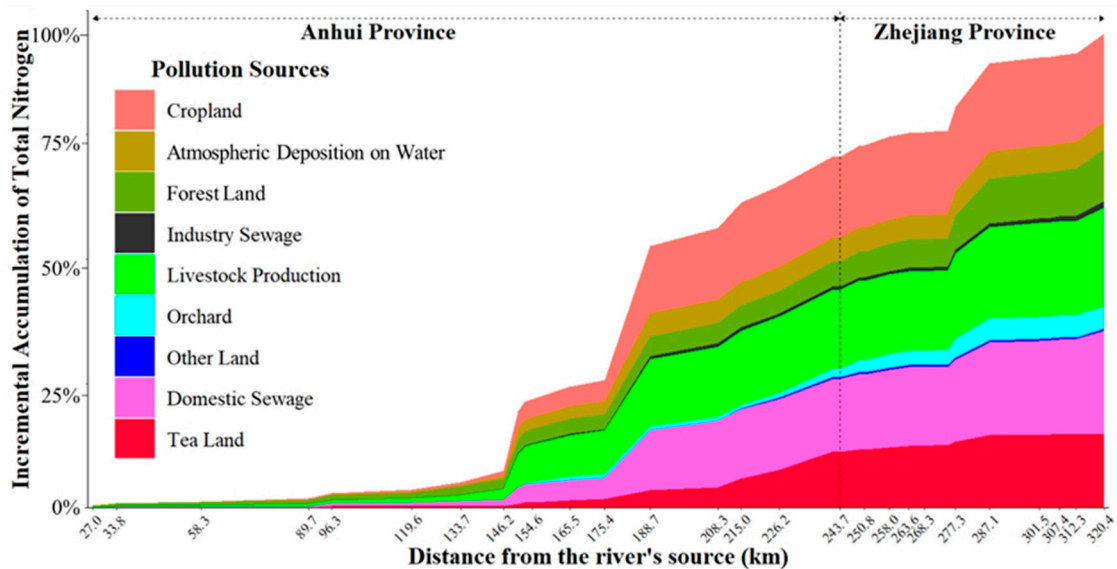
Figure 7. Average annual contributions of point and non-point sources of TN pollution along the main reach of the Xin'anjiang River.

A second, even sharper surge in TN is at location 188.7 km, near a tributary that flows through the municipalities of Shexian and Huizhou (both part of Huangshan City) and nearby highly populated areas before entering the Xin'anjiang River. Significant increases in TN attributable to domestic sewage

are evident at this site. Downstream TN pollution from all sources then increases gradually until a third surge appears at location 287.1 km in Zhejiang Province. Elevated TN discharge from highly erodible forested slopes [2], and to a lesser extent from domestic sewage and orchard, are major contributors to the increase at this location. Distinct spatial patterns of TN release from plant-based agriculture are clearly evident along the course of the river. Thus, the accumulation of TN from cropland and tea land reaches its near maximum before the Xin'anjiang River flows out of Anhui Province, but most of the TN accumulation from orchard land occurs later, as the river flows through Zhejiang Province.

Delivery of TN from non-point sources to the Xin'anjiang River can follow three general pathways: lateral flow, groundwater, and surface flow. The contributions of these pathways to TN accumulation in the river are visualized in Figure 8, which reveals four significant surges of TN from non-point sources and identifies spatially explicit contributions of lateral flow, groundwater, and surface water. The first surge, at Tunxi (location 154.6 km), is primarily attributable to increases from surface flow and groundwater, but the second, at location 208.3 km, is primarily attributable to increases in lateral and surface flow. The third and fourth surges peak at Jiekou, on the border between the provinces (location 243.7 km) and within Zhejiang Province (location 287.1 km), respectively. Almost all of the incremental increase at both of these locations is contributed by lateral flow, which ultimately accounted for nearly two-thirds of TN transport in the river.
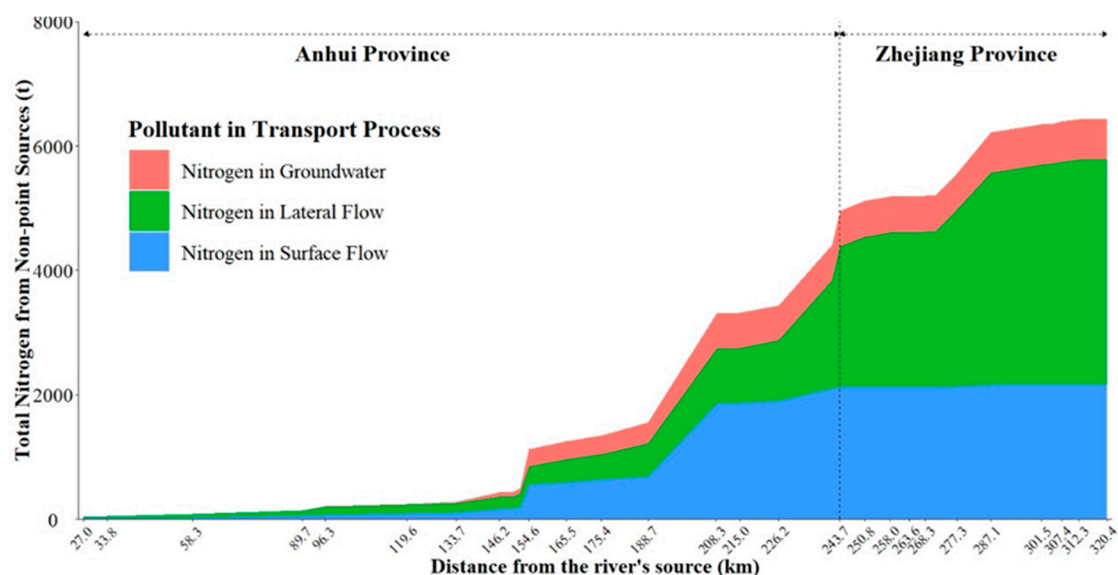
Figure 8. Average annual contributions of non-point sources of TN pollution along the main reach of the Xin'anjiang River.

The monthly dynamics of TN discharge from non-point sources via groundwater, surface flow, and lateral flow (Figure 9) generally correspond to monthly rainfall (Figure 4). Release of TN is most significant from February through August and sharply reduced during the other months, when TN from groundwater and surface flows become insignificant. Lateral flow and surface flow transport roughly equivalent amounts of TN during the period of peak movement, except for February and March, when lateral flow predominates and exceeds the contribution from surface flow by three to four-fold. Groundwater movement of TN, on the other hand, increases progressively during this same period, but is of minor significance compared to the other two pathways.
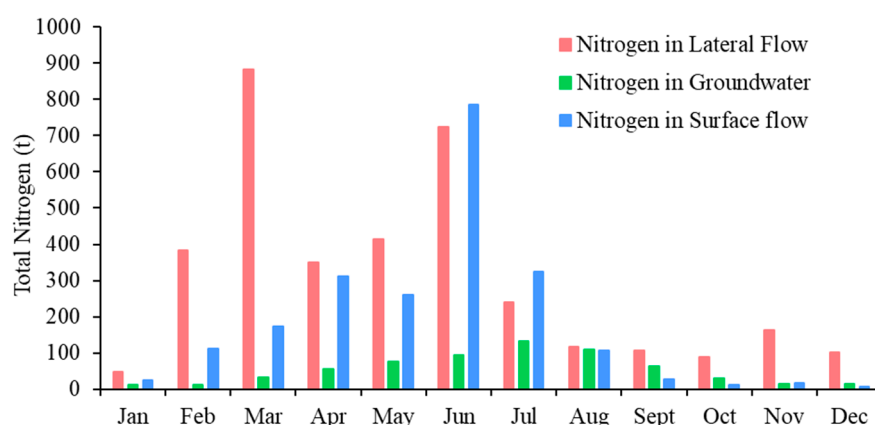
Figure 9. Monthly dynamics of TN movement via three different non-point source routes.

4. Discussion

4.1. Spatio-Temporal Dynamics of TN Transport

The QLB is characterized by hilly topography, diverse, rapidly intensifying agricultural production, and several urban areas where domestic and industrial activities are concentrated [25,31]. It is no wonder, then, that nutrient pollution in the basin is governed by dynamic upstream to downstream transport processes that are spatially and temporally heterogeneous and poorly understood [24,49]. It has been known for several decades that these factors have seriously compromised water quality in the basin [27]. China's first transboundary Payment for Ecosystem Services (PES) plan was consequently established in the QLB in 2012 [50,51]. Although this scheme has generated significant investment to reduce nutrient pollution entering the lower basin from Anhui Province, many fundamental questions persist, and water quality in the Xin'anjiang River and Qiandao Lake remains at risk [31,52].

Here a modeling approach scaled to the entire QLB was employed to understand the spatiotemporal dynamics of TN, a key polluting nutrient in both hilly [44,49,53,54] and lowland basins [55,56]. We establish that TN from point sources, which is almost equally attributable to livestock production and domestic sewage, accounts for nearly half of the aggregate TN loads in the basin. Both of these point sources are longstanding targets for mitigation under the PES plan [51]. On the other hand, seasonal surface and lateral flows from non-point sources account for the majority of TN loads in the QLB, with crop, tea, and orchard lands together comprising nearly 40% of the total. The yield of TN from tea land exceeds that from other crop types, and although crop production is declining in the area [57,58], tea cultivation is rapidly expanding, both in the QLB and in other nearby basins with similar topography [27,31,59,60]. This is important because agricultural fertilizers are commonly applied in excessive amounts to tea and other intensively managed crops in the basin, especially the upper basin in Anhui Province [59–63].

In general, incremental contributions of TN from non-point sources in the lower basin rise modestly and proportionately to one another, but disproportionately high contributions are evident from forest land and orchards in Zhejiang Province [31,59]. The dynamics differ, however, because forest land contributes high TN loads but low TN yields, but the situation is reversed with orchard land, which contributes low TN loads but high TN yields. The significant degree of forest coverage in the QLB contributes to high TN loads [27], but slope and erosion are also major factors. The mean slope of the study area is 24.9°, and the area proportions of slopes < 10°, 10°–20°, 20°–25°, 25°–30°, and >30° are 22%, 13%, 9%, 12%, and 44%, respectively. Sediment loss from such highly erodible forested slopes in the QLB is known to be substantial [44], and the importance of these sediments in the release of TN is documented [57]. In contrast, orchards are currently a minor but growing land use category in the QLB. Our data underscore the need for further study of their role in nutrient pollution in the basin.

Not all sub-basins in a given catchment contribute equally to nutrient loads, even if they are similar [55,56,64]. Nutrient runoff is known to be sensitive to mountainous topography and abundant annual rainfall in eastern China [44], and the differential influence of steeper and flatter lands on seasonal variation of nutrient loads is well documented [55,56]. We found that sub-basin to sub-basin heterogeneity in TN loads and yields was pronounced across the QLB, where four clustered sub-basins located upstream in Anhui Province stand out as a hotspot, because of their extensive and intensive contributions to TN pollution. These adjacent sub-basins deliver high annual TN loads ranging from 423 to 576 t and correspondingly high TN yields that can be as high as 5.3 t/km^2/yr. Similar TN loads characterize a few other areas of the QLB, including the large sub-basin surrounding Qiandao Lake, where the annual contribution is 464 t. TN yields in these areas are nevertheless modest (just 0.4 t/km^2/yr in the case of the sub-basin surrounding Qiandao Lake).

There are two important practical reasons to assign significance to pollution hotspots such as those identified here in the QLB. First, hotspots represent priority areas for detailed analysis of factors that contribute to TN pollution, e.g., soils, land use patterns (including legacy effects), agronomic management procedures, and topographical features such as hillslopes and streams that affect movement of nutrients [65–71]. Second, hotspots are locations where efforts to control pollution are likely to be most efficient and have the greatest impacts [31,59]. Knowledge of their location and characteristics is especially relevant in the QLB, where significant ongoing investments are underway to reduce transport of TN into Qiandao Lake [72,73].

Although pathways of nutrient transport have been examined in the QLB [10,27] and other hilly areas of eastern China [74–76], the proportion of pollution contamination from surface flow, sub-surface flow, and groundwater is difficult to monitor in field experiments [77]. Physical-based modeling with multivariate correlated data as employed here is consequently useful, because it can spatially resolve the relative contributions of TN transport processes. These dynamics are illustrated with the Xin'anjiang River, where, for example, modeling revealed that TN loads from nonpoint sources doubled over a distance of less than 10 km (between locations 146.2 and 154.6 km, see Figure 8). Although groundwater was a relatively significant transport component at this location, surface and lateral flow assumed increasing importance as the river flowed downstream, such that the overall significance of groundwater was eventually marginalized.

The relative contributions of lateral and surface flow to TN also changed as the river flowed downstream, i.e., the incremental contribution of lateral flow rose continuously after the river passed beyond location 154.6 km, but that of surface flow nearly ceased before the river entered Zhejiang Province at location 243.7 km. Thereafter, almost all incremental increase in TN was due to lateral flow, which would be expected to be significant in this area, which is characterized by dense agriculture and disturbed soils capable of enhancing such flows. The above insights from basin-wide analysis underscore the importance of this perspective, which can amplify more detailed information obtained from narrowly focused studies of sub-basins [27].

4.2. The Basin's N Cycle and Implications for Pollution Management

Figure 10 shows the integrated N cycle for the QLB as simulated by the SWAT model used here. Net N intake is assigned to three non-point sources (in decreasing order of magnitude: fertilizer, N stored in the soil, and atmospheric deposition) and three point sources (in decreasing order of magnitude: domestic sewage, livestock production, and industrial sewage). The most significant N outlet in the terrestrial area consists of processes associated with plant growth, e.g., N removal via harvest of agricultural crops, but processes such as ammonia volatilization, denitrification, and the return of N from plant litter to the soil are also important [78]. Thirteen percent of N from non-point sources in the basin is discharged into water bodies (Figure 10). This amount exceeds that discharged from point sources in the QLB and on a percentage basis, it is much greater than the 1.8%–4.5% determined earlier in a nearby low hilly basin with humid climate [79]. Entry of N from non-point

sources thus represents a major environmental concern, even though nearly one-quarter of the N is removed from the basin's waterways during transport.
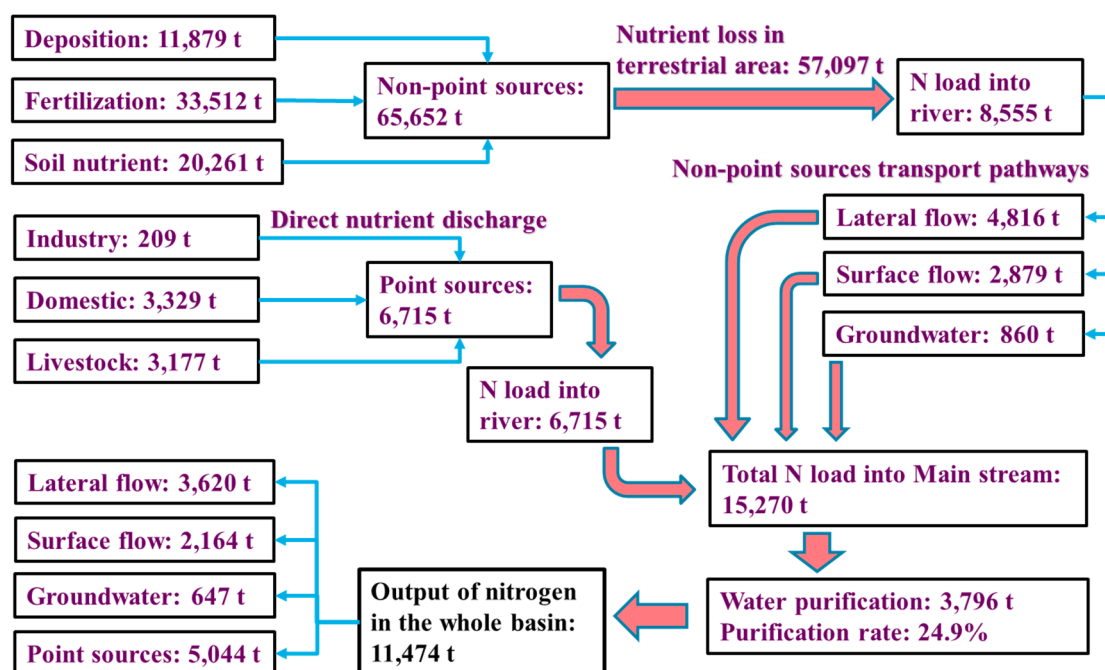
Figure 10. Diagrammatic representation of the area-averaged N budget of the QLB during the period from 2007 to 2016. Blue arrows represent net N inputs and pink arrows represent net N outlets and in-basin consumption. Note that rainfall N deposition here represents all deposition from every land use across the basin, including the water body component.

Key parameters of streamflow and N transport (Table 1), as well as the relatively small Manning 'n' value, the percolation coefficient, and transmission loss to the deep aquifer (Table 2), highlight the significance of subsurface flow in the QLB. Such flow is facilitated by shallow soils and frequent heavy rainfall events in basins with steep topography and convex hillsides [80], and it represents the main N delivery pathway and thus the principal target for reducing N pollution in the QLB. Consistent with the view that agricultural land and associated N fertilizer inputs are key factors for protecting aquatic environments [10,27,81,82], the control of N pollution in the QLB and similar basins currently emphasizes reduced fertilization, application of controlled-release fertilizers, construction of waste water treatment plants, collection of livestock sewage, and restriction of agricultural development [83]. On the basis of SWAT modeling, a strategy which has previously been employed to identify ways to reduce pollutant loads in other regions [84,85], we suggest a shift from controlling N loads to a targeted and comprehensive strategy emphasizing N distribution and transport processes.

Our SWAT analysis draws attention to two key factors for nutrient management in the QLB. The first is temporal and indicates that processes occurring during the period before June, especially those that influence subsurface flows in March, are crucial for annual N output. The second is spatial and emphasizes the importance of hotspots in the basin that contribute disproportionately to N outputs. These factors underscore the importance of restriction of agriculture on steep slopes—especially intensive agriculture that often relies on heavy applications of fertilizers in the spring. They also highlight the need for effective sewage collection—especially strategies that minimize N in tail water discharge, a goal that has proved elusive in the past [2,27,44].

Lakeside buffers [86,87], maintenance of high fractional vegetation cover [88,89], and construction of ponds to slow water movement and intercept nutrients [60] during the rainy season would undoubtedly reduce N loss in the QLB. The health of the basin's riparian and aquatic ecosystem could

be further improved by adopting soil and water conservation strategies such as the restoration of vegetation and construction of wetlands. A third option involves the establishment of an ecological interception system to disrupt the N delivery pathway from subsurface flow to the lake and the basin's major waterways. Measures such as vegetative filter strips and ecological interception ditches would exploit chemical and biological mechanisms of self-purification and N retention to promote effective N reduction in the ecosystem [31,59,90].

5. Conclusions

Complex topographical conditions, varying climatic factors, and intensive anthropogenic activities exacerbate N pollution in hilly basins with monsoon climate. Understanding of source apportionment and spatiotemporal dynamics of N distribution and transportation is consequently vital for formulating reasonable strategies to ensure comprehensive water quality management in these basins. The physical-based SWAT model was utilized in this study to simulate the drivers and transport process of N, so that effective nutrient management of the QLB can be facilitated. Three main conclusions can be drawn.

First, optimization of localized model parameters suitable for hilly areas with monsoon climate enables the SWAT model to provide reliable estimates of N loads in the basin. The model confirms that, owing to the shallow soil layer and intensive rainfall, N loss from subsurface flow in the period before rainy season is the main driver of the N transport process. Complex terrain and severe rainfall heterogeneity enhance the complexity of the problem.

Second, non-point sources are the major contributors to N loads across the QLB, with cropland, tea land, and the basin's extensive tracts of highly erodible forest land accounting for 18%, 15%, and 10% of the TN loads, respectively. Major point sources include domestic sewage (21%) and livestock production (20%). The basin is characterized by the existence of hotspot sub-basins of high TN yield, non-uniform loading of TN along the reach of the Xin'anjiang River, and spatially determined variability in the relative contributions of different transport processes to TN movement.

Third, physical-based modeling suggests that N pollution control in the QLB can be made more comprehensive and efficient. Upstream to downstream analysis of the N transport pathway highlights the need not only to construct more wastewater treatment plants in areas identified here as sites of high domestic and industrial pollution, but also to increase their operational efficiency. In addition, soil and water conservation practices should be targeted to areas identified here with intensive agriculture and high TN yields. Insights from this study thus are likely to aid regional management of the QLB and provide a framework for similar monsoon basins elsewhere.

Supplementary Materials: The following are available online at http://www.mdpi.com/2073-4441/12/4/1075/s1. Figure S1: Land use classes used for SWAT analysis of the Qiandao Lake basin, Figure S2: The soil types map of the Qiandao Lake basin that was generated for use in SWAT analysis, Figure S3: Temporal and spatial heterogeneity of precipitation as recorded by individual rainfall stations (dots) compared to that recorded at two meteorological stations (dashed lines), Table S1: Fertilization and other agricultural management operations, Table S2: Main localized crop parameters of tea land.

Author Contributions: Conceptualization: D.C. and H.L.; methodology: D.C., W.Z., and J.P.; software, validation, and formal analysis: D.C.; investigation, resources, and data curation: D.C. and Y.D.; writing—original draft preparation: D.C.; writing, review, and editing: D.C., H.L., W.Z. and S.G.P. All authors have read and agreed to the published version of the manuscript.

Funding: This research was funded by an Agricultural and Social Development Project of Hangzhou, Zhejiang Province, grant number [20180417A06], the National Natural Science Foundation, grant number [41877513], the National Key R&D Program of China [2018YFD1100102], and the Thirteenth Five-Year Plan of the Nanjing Institute of Geography and Limnology [NIGLAS2018GH06].

Acknowledgments: The authors wish to express their gratitude to the Environmental Protection Agency of Chun'an and the Hangzhou Environmental Protection Research Institute for funding the collaboration that generated this paper. S.G.P. acknowledges the Nanjing Agricultural University-Michigan State University Asia Hub Program for supporting his participation in the investigation. We thank Weimin Chen, Zhixu Wu, and Yicai Han for insights on aquatic management, and Pengcheng Li, Jianwei Geng, and Wenyan Lu for advice, encouragement, and support.

Conflicts of Interest: The authors declare no conflict of interest.

References

1. Markogianni, V.; Mentzafou, A.; Dimitriou, E. Assessing the impacts of human activities and soil erosion on the water quality of Plastira mountainous Mediterranean Lake, Greece. *Environ. Earth Sci.* **2016**, *75*, 915. [CrossRef]
2. Wang, X.; Wang, Q.; Wu, C.; Liang, T.; Zheng, D.; Wei, X. A method coupled with remote sensing data to evaluate non-point source pollution in the Xin'anjiang catchment of China. *Sci. Total Environ.* **2012**, *430*, 132–143. [CrossRef] [PubMed]
3. Nayyeri, H.; Zandi, S. Evaluation of the effect of river style framework on water quality: Application of geomorphological factors. *Environ. Earth Sci.* **2018**, *77*, 343. [CrossRef]
4. Wang, H.; Wu, Z.; Hu, C. A Comprehensive Study of the Effect of Input Data on Hydrology and non-point Source Pollution Modeling. *Water Resour. Manag.* **2015**, *29*, 1505–1521. [CrossRef]
5. Zhou, P.; Huang, J.; Hong, H. Modeling nutrient sources, transport and management strategies in a coastal watershed, Southeast China. *Sci. Total Environ.* **2018**, *610–611*, 1298–1309. [CrossRef] [PubMed]
6. Hu, M.; Liu, Y.; Wang, J.; Dahlgren, R.A.; Chen, D. A modification of the Regional Nutrient Management model (ReNuMa) to identify long-term changes in riverine nitrogen sources. *J. Hydrol.* **2018**, *561*, 31–42. [CrossRef]
7. Que, Z.; Seidou, O.; Droste, R.L.; Wilkes, G.; Sunohara, M.; Topp, E.; Lapen, D.R. Using AnnAGNPS to Predict the Effects of Tile Drainage Control on Nutrient and Sediment Loads for a River Basin. *J. Environ. Qual.* **2015**, *44*, 629–641. [CrossRef]
8. Mishra, B.K.; Regmi, R.K.; Masago, Y.; Fukushi, K.; Kumar, P.; Saraswat, C. Assessment of Bagmati river pollution in Kathmandu Valley: Scenario-based modeling and analysis for sustainable urban development. *Sustain. Water Qual. Ecol.* **2017**, *9–10*, 67–77. [CrossRef]
9. Wang, Q.; Xu, Y.; Xu, Y.; Wu, L.; Wang, Y.; Han, L. Spatial hydrological responses to land use and land cover changes in a typical catchment of the Yangtze River Delta region. *Catena* **2018**, *170*, 305–315. [CrossRef]
10. Zhang, Y.; Lan, J.; Li, H.; Liu, F.; Luo, L.; Wu, Z.; Yu, Z.; Liu, M. Estimation of external nutrient loadings from the main tributary (Xin'anjiang) into Lake Qiandao, 2006–2016. *J. Lake Sci.* **2019**, *31*, 1534–1546. (In Chinese)
11. Arnold, J.G.; Fohrer, N. SWAT2000: Current capabilities and research opportunities in applied watershed modelling. *Hydrol. Process.* **2005**, *19*, 563–572. [CrossRef]
12. Luzio, M.D.; Srinivasan, R.; Arnold, J.G. A GIS-Coupled Hydrological Model System for the Watershed Assessment of Agricultural Nonpoint and Point Sources of Pollution. *Trans. GIS* **2010**, *8*, 113–116. [CrossRef]
13. Cerro, I.; Antiguedad, I.; Srinavasan, R.; Sauvage, S.; Volk, M.; Sanchez-Perez, J.M. Simulating land management options to reduce nitrate pollution in an agricultural watershed dominated by an alluvial aquifer. *J. Environ. Qual.* **2014**, *43*, 67–74. [CrossRef] [PubMed]
14. Withers, P.J.A.; May, L.; Jarvie, H.P.; Jordan, P.; Doody, D.; Foy, R.H.; Bechmann, M.; Cooksley, S.; Dils, R.; Deal, N. Nutrient emissions to water from septic tank systems in rural catchments: Uncertainties and implications for policy. *Environ. Sci. Policy* **2012**, *24*, 71–82. [CrossRef]
15. Malago, A.; Bouraoui, F.; Vigiak, O.; Grizzetti, B.; Pastori, M. Modelling water and nutrient fluxes in the Danube River Basin with SWAT. *Sci. Total Environ.* **2017**, *603–604*, 196–218. [CrossRef] [PubMed]
16. Nguyen, H.H.; Recknagel, F.; Meyer, W.; Frizenschaf, J.; Shrestha, M.K. Modelling the impacts of altered management practices, land use and climate changes on the water quality of the Millbrook catchment-reservoir system in South Australia. *J. Environ. Manag.* **2017**, *202*, 1–11. [CrossRef]
17. Maharjan, G.R.; Park, Y.S.; Kim, N.; Shin, D.S.; Choi, J.; Hyun, G.; Jeon, J.-H.; Ok, Y.S.; Lim, K.J. Evaluation of SWAT sub-daily runoff estimation at small agricultural watershed in Korea. *Front. Environ. Sci. Eng.* **2013**, *7*, 109–119. [CrossRef]
18. Glavan, M.; White, S.; Holman, I.P. Evaluation of River Water Quality Simulations at a Daily Time Step—Experience with SWAT in the Axe Catchment, UK. *Clean-Soil AirWater* **2011**, *39*, 43–54. [CrossRef]
19. Tuppad, P.; Douglas-Mankin, K.R.; Koelliker, J.K.; Hutchinson, J.M.S. SWAT Discharge Response to Spatial Rainfall Variability in a Kansas Watershed. *Trans. ASABE* **2010**, *53*, 65–74. [CrossRef]
20. Yang, X.; Warren, R.; He, Y.; Ye, J.; Li, Q.; Wang, G. Impacts of climate change on TN load and its control in a River Basin with complex pollution sources. *Sci. Total Environ.* **2018**, *615*, 1155–1163. [CrossRef]

21. Shao, G.; Guan, Y.; Zhang, D.; Yu, B.; Zhu, J. The Impacts of Climate Variability and Land Use Change on Streamflow in the Hailiutu River Basin. *Water* **2018**, *10*, 814. [CrossRef]

22. Zhang, H.; Peng, S.; Zhou, Y.; Yuan, H.; Chen, J. Analysis of current pollutant loads and investigation of total pollutant discharge limits in Qiandao Lake. *Water Resour. Prot.* **2014**, *30*, 53–56. (In Chinese)

23. MEP. *Chinese Environmental Quality Standards for Surface Water (GB 3838-2002)*; Ministry of Environmental Protection of the People's Republic of China: Beijing, China, 2002. (In Chinese)

24. Da, W.; Li, Y.; Zhu, G.; Xu, H.; Liu, M.; Lan, J.; Wang, Y.; WU, Z.; Zheng, W. Influence of Hydrometeorological Process on Nutrient Dynamics in Qiandao Lake. *J. Hydroecol.* **2019**, *40*, 9–19. (In Chinese)

25. Han, X.; Zhu, G.; Wu, Z.; Chen, W.; Zhu, M. Spatial-temporal variations of water quality parameters in Xin'anjiang Reservoir (Lake Qiandao) and the water protection strategy. *J. Lake Sci.* **2013**, *25*, 836–845. (In Chinese)

26. Wu, Z.; Liu, M.; Lan, J.; He, J.; Yu, Z. Vertical distribution of phytoplankton and physico-chemical characteristics in the lacustrine zone of Xin'anjiang Reservoir(Lake Qiandao) in subtropic China during summer stratification. *J. Lake Sci.* **2012**, *24*, 460–465. (In Chinese)

27. Li, Z.; Liu, M.; Zhao, Y.; Liang, T.; Sha, J.; Wang, Y. Application of Regional Nutrient Management Model in Tunxi Catchment: In Support of the Trans-boundary Eco-compensation in Eastern China. *Clean-Soil Air Water* **2014**, *42*, 1729–1739. [CrossRef]

28. FAO. *The World Fertilizer Outlook*; Food and Agriculture Organization of the United Nations: Rome, Italy, 2015.

29. Gao, T.; Xie, L.; Liu, B. Association of extreme precipitation over the Yangtze River Basin with global air-sea heat fluxes and moisture transport. *Int. J. Climatol.* **2016**, *36*, 3020–3038. [CrossRef]

30. Wang, R.; Chen, J.; Chen, X.; Wang, Y. Variability of precipitation extremes and dryness/wetness over the southeast coastal region of China, 1960–2014. *Int. J. Climatol.* **2017**, *37*, 4656–4669. [CrossRef]

31. Pueppke, S.G.; Zhang, W.; Li, H.; Chen, D.; Ou, W. An Integrative Framework to Control Nutrient Loss: Insights from Two Hilly Basins in China's Yangtze River Delta. *Water* **2019**, *11*, 2036. [CrossRef]

32. MWR. *Hydrological Data of River Basins in China*; Ministry of Water Resources of China: Beijing, China, 2016. (In Chinese)

33. CBS. *Chun'an Statistical Yearbook*; Chun'an Bureau of Statistic, China: Hangzhou, China, 2016. (In Chinese)

34. HBS. *Huangshan Statistical Yearbook*; Huangshan Bureau of Statistic, China: Huangshan, China, 2016. (In Chinese)

35. Uniyal, B.; Jha, M.K.; Verma, A.K. Assessing Climate Change Impact on Water Balance Components of a River Basin Using SWAT Model. *Water Resour. Manag.* **2015**, *29*, 4767–4785. [CrossRef]

36. Abbaspour, K.C.; Rouholahnejad, E.; Vaghefi, S.; Srinivasan, R.; Yang, H.; Kløve, B. A continental-scale hydrology and water quality model for Europe: Calibration and uncertainty of a high-resolution large-scale SWAT model. *J. Hydrol.* **2015**, *524*, 733–752. [CrossRef]

37. Luo, P.; Zhou, M.; Deng, H.; Lyu, J.; Cao, W.; Takara, K.; Nover, D.; Geoffrey Schladow, S. Impact of forest maintenance on water shortages: Hydrologic modeling and effects of climate change. *Sci. Total Environ.* **2018**, *615*, 1355–1363. [CrossRef] [PubMed]

38. Nash, J.E.; Sutcliffe, J.V. River flow forecasting through conceptual models, part I. A discussion of principles. *J. Hydrol.* **1970**, *10*, 282–290. [CrossRef]

39. Moriasi, D.N.; Arnold, J.G.; Liew, M.W.V.; Bingner, R.L.; Harmel, R.D.; Veith, T.L. Model Evaluation Guidelines for Systematic Quantification of Accuracy in Watershed Simulations. *Trans. ASABE* **2007**, *50*, 885–900. [CrossRef]

40. Du, X.; Shrestha, N.K.; Wang, J. Assessing climate change impacts on stream temperature in the Athabasca River Basin using SWAT equilibrium temperature model and its potential impacts on stream ecosystem. *Sci. Total Environ.* **2019**, *650*, 1872–1881. [CrossRef]

41. Shen, Z.Y.; Gong, Y.W.; Li, Y.H.; Hong, Q.; Xu, L.; Liu, R.M. A comparison of WEPP and SWAT for modeling soil erosion of the Zhangjiachong Watershed in the Three Gorges Reservoir Area. *Agric. Water Manag.* **2009**, *96*, 1435–1442. [CrossRef]

42. Han, L.; Huang, M.; Ma, M.; Wei, J.; Hu, W.; Chouhan, S. Evaluating sources and processing of nonpoint source nitrate in a small suburban watershed in China. *J. Hydrol.* **2018**, *559*, 661–668. [CrossRef]

43. Zhang, M.K.; Xu, J.M. Restoration of surface soil fertility of an eroded red soil in southern China. *Soil Tillage Res.* **2005**, *80*, 13–21. [CrossRef]

44. Zhai, X.; Zhang, Y.; Wang, X.; Xia, J.; Liang, T. Non-point source pollution modelling using Soil and Water Assessment Tool and its parameter sensitivity analysis in Xin'anjiang catchment, China. *Hydrol. Process.* **2014**, *28*, 1627–1640. [CrossRef]

45. Tuo, Y.; Duan, Z.; Disse, M.; Chiogna, G. Evaluation of precipitation input for SWAT modeling in Alpine catchment: A case study in the Adige river basin (Italy). *Sci. Total Environ.* **2016**, *573*, 66–82. [CrossRef]

46. Campling, P.; Gobin, A.; Feyen, J. Temporal and spatial rainfall analysis across a humid tropical catchment. *Hydrol. Process.* **2001**, *15*, 359–375. [CrossRef]

47. Lan, J.; Wang, Y.; Chen, S.; Yu, C.; Wu, Z.; Zhang, Y. Time Variation Characteristics of the Main Inflow Nutrient at Xin'anjiang Reservoir and Its Impact factors in 2007–2016. *Environ. Monit. China* **2019**, *35*, 95–101. (In Chinese)

48. Sonnenborg, T.O.; Hinsby, K.; van Roosmalen, L.; Stisen, S. Assessment of climate change impacts on the quantity and quality of a coastal catchment using a coupled groundwater–surface water model. *Clim. Chang.* **2011**, *113*, 1025–1048. [CrossRef]

49. Wen, J.; Luo, D.; Luo, X.; Tang, D.; Chen, S. Agriculture non-point source pollution control measures of Qiandao lake area. *J. Soil Water Conserv.* **2004**, *18*, 126–129. (In Chinese)

50. FAO. *Case Studies on Remuneration of Positive Externalities (RPE)*; Payments for Environmental Services (PES): Rome, Italy, 2013.

51. Wang, J.; Wang, Y.; Liu, G.; Zhao, Y. The first eco-compensation for crossing provinces of downstream and upstream in China: A model of Xinanjiang River. *Environ. Prot.* **2016**, *14*, 38–40. (In Chinese) [CrossRef]

52. Chen, P.; Mao, Z.; Zhang, Z.; Liu, H.; Pan, D. Detecting subsurface phytoplankton layer in Qiandao Lake using shipborne lidar. *Opt. Express* **2020**, *28*, 558. [CrossRef]

53. Peterson, B.J.; Wollheim, W.M.; Mulholland, P.J.; Webster, J.R.; Meyer, J.L.; Tank, J.L.; Marti, E.; Bowden, W.B.; Valett, H.M.; Hershey, A.E.; et al. Control of nitrogen export from watersheds by headwater streams. *Science* **2001**, *292*, 86–90. [CrossRef]

54. Xia, J.; Zhang, Y.-Y.; Zhan, C.; Ye, A.Z. Water Quality Management in China: The Case of the Huai River Basin. *Int. J. Water Resour. Dev.* **2011**, *27*, 167–180. [CrossRef]

55. Yu, S.; Xu, Z.; Wu, W.; Zuo, D. Effect of land use types on stream water quality under seasonal variation and topographic characteristics in the Wei River basin, China. *Ecol. Indic.* **2016**, *60*, 202–212. [CrossRef]

56. Wan, R.; Cai, S.; Li, H.; Yang, G.; Li, Z.; Nie, X. Inferring land use and land cover impact on stream water quality using a Bayesian hierarchical modeling approach in the Xitiaoxi River Watershed, China. *J. Environ. Manag.* **2014**, *133*, 1–11. [CrossRef]

57. Jia, X.; Luo, W.; Wu, X.; Wei, H.; Wang, B.; Phyoe, W.; Wang, F. Historical record of nutrients inputs into the Xin'an Reservoir and its potential environmental implication. *Environ. Sci. Pollut. Res. Int.* **2017**, *24*, 20330–20341. [CrossRef] [PubMed]

58. Yang, G. Land use and land cover change and regional economic development: The revelation of the change in cropland area in the Yangtze River delta during the past 50 years. *Acta Geogr. Sin.* **2004**, *59*, 41–46. (In Chinese)

59. Li, H.; Chen, W.; Yang, G.; Nie, X. Reduction of nitrogen and phosphorus emission and zoning management targeting at water quality of lake or reservoir systems: A case study of Shahe Reservoir within Tianmuhu Reservoir area. *J. Lake Sci.* **2013**, *25*, 785–798. (In Chinese)

60. Zhang, W.; Li, H.; Pueppke, S.; Diao, Y.; Nie, X.; Geng, J.; Chen, D.; Pang, J. Nutrient loss is sensitive to land cover changes and slope gradients of agricultural hillsides: Evidence from four contrasting pond systems in a hilly catchment. *Agric. Water Manag.* **2020**, in press.

61. Xu, Q. The Study of Agricultural Non-Point Source Pollution Control Policy System. Master's Thesis, Michigan Technological University, Houghton, MI, USA, 2014.

62. Li, X.; Zhang, L.; Yang, G.; Li, H.; He, B.; Chen, Y.; Tang, X. Impacts of human activities and climate change on the water environment of Lake Poyang Basin, China. *Geoenviron. Disasters* **2015**, *2*. [CrossRef]

63. Han, Y.; Li, H.; Nie, X.; Xu, X. Nitrogen and phosphorus budget of different land use types in hilly area of Lake Taihu upper river basin. *J. Lake Sci.* **2012**, *24*, 829–837. (In Chinese)

64. Beven, K.; Heathwaite, L.; Haygarth, P.; Walling, D.; Brazier, R.; Withers, P. On the concept of delivery of sediment and nutrients to stream channels. *Hydrol. Process.* **2005**, *19*, 551–556. [CrossRef]

65. Gao, W.; Howarth, R.W.; Hong, B.; Swaney, D.P.; Guo, H.C. Estimating net anthropogenic nitrogen inputs (NANI) in the Lake Dianchi basin of China. *Biogeosciences* **2014**, *11*, 4577–4586. [CrossRef]

66. Tomer, M.D.; Moorman, T.B.; Kovar, J.L.; Cole, K.J.; Nichols, D.J. Eleven years of runoff and phosphorus losses from two fields with and without manure application, Iowa, USA. *Agric. Water Manag.* **2016**, *168*, 104–111. [CrossRef]

67. Vadas, P.A.; Powell, J.M. Monitoring nutrient loss in runoff from dairy cattle lots. *Agric. Ecosyst. Environ.* **2013**, *181*, 127–133. [CrossRef]

68. Potter, T.L.; Bosch, D.D.; Strickland, T.C. Tillage impact on herbicide loss by surface runoff and lateral subsurface flow. *Sci. Total Environ.* **2015**, *530–531*, 357–366. [CrossRef] [PubMed]

69. Alexander, R.B.; Boyer, E.W.; Smith, R.A.; Schwarz, G.E.; Moore, R.B. The Role of Headwater Streams in Downstream Water Quality. *J. Am. Water Resour. Assoc.* **2007**, *43*, 41–59. [CrossRef] [PubMed]

70. Suescún, D.; Villegas, J.C.; León, J.D.; Flórez, C.P.; García-Leoz, V.; Correa-Londoño, G.A. Vegetation cover and rainfall seasonality impact nutrient loss via runoff and erosion in the Colombian Andes. *Reg. Environ. Chang.* **2016**, *17*, 827–839. [CrossRef]

71. Lai, X.; Zhu, Q.; Zhou, Z.; Liao, K.; Lv, L. Optimizing the spatial pattern of land use types in a mountainous area to minimize non-point nitrogen losses. *Geoderma* **2020**, *360*, 114016. [CrossRef]

72. Zhang, W.; Swaney, D.P.; Hong, B.; Howarth, R.W.; Han, H.; Li, X. Net anthropogenic phosphorus inputs and riverine phosphorus fluxes in highly populated headwater watersheds in China. *Biogeochemistry* **2015**, *126*, 269–283. [CrossRef]

73. ZPMF. *Horizontal Ecological Compensation Agreement for Upstream and Downstream of Xinanjiang River Basin*; Zhejiang Provincial Ministry of Finance: Hangzhou, China, 2018. (In Chinese)

74. Zheng, H.; Liu, Z.; Zuo, J.; Wang, L.; Nie, X. Characteristics of Nitrogen Loss through Surface-Subsurface Flow on Red Soil Slopes of Southeast China. *Eurasian Soil Sci.* **2018**, *50*, 1506–1514. [CrossRef]

75. Wu, X.; Zhang, L.; Zhang, M.; Ni, H.; Wang, H. Research on characteristics of nitrogen loss in sloping land under different rainfall intensities. *Acta Geogr. Sin.* **2007**, *27*, 4576–4582. (In Chinese)

76. Chen, X.; Yang, J.; Zheng, T.; Zhang, J. Sediment, runoff, nitrogen and phosphorus losses of sloping cropland of quaternary red soil in Northern Jiangxi. *Trans. Chin. Soc. Agric. Eng.* **2015**, *31*, 162–167. (In Chinese) [CrossRef]

77. Lane, S.N.; Reaney, S.M.; Heathwaite, A.L. Representation of landscape hydrological connectivity using a topographically driven surface flow index. *Water Resour. Res.* **2009**, *45*. [CrossRef]

78. Wang, P.; Sadeghi, A.; Linker, L.; Arnold, J.; Shenk, G.; Wu, J. Simulated soil water content effect on plant nitrogen uptake and export in watershed management. In *Quantifying and Understanding Plant Nitrogen Uptake for Systems Modeling*; Ma, L., Ahuja, L.R., Bruulsema, T., Eds.; CRC Press: Boca Raton, FL, USA, 2009; pp. 277–304.

79. Zhang, W.; Li, H.; Li, Y. Spatio-temporal dynamics of nitrogen and phosphorus input budgets in a global hotspot of anthropogenic inputs. *Sci. Total Environ.* **2019**, *656*, 1108–1120. [CrossRef]

80. Freeze, R.A. Role of subsurface flow in generating surface runoff. 2. Upstream source areas. *Water Resour. Res.* **1972**, *8*, 1272–1283. [CrossRef]

81. Zhang, W.; Li, H.; Kendall, A.D.; Hyndman, D.W.; Diao, Y.; Geng, J.; Pang, J. Nitrogen transport and retention in a headwater catchment with dense distributions of lowland ponds. *Sci. Total Environ.* **2019**, *683*, 37–48. [CrossRef] [PubMed]

82. Weigelhofer, G.; Hein, T.; Bondar-Kunze, E. Phosphorus and nitrogen dynamics in riverine systems: Human impacts and management options. In *Riverine Ecosystem Management*; Scmutz, S., Sendzimir, J., Eds.; Springer: Cham, Switzerland, 2018; pp. 187–202.

83. Yang, X.; Fang, S. Practices, perceptions, and implications of fertilizer use in East-Central China. *Ambio* **2015**, *44*, 647–652. [CrossRef] [PubMed]

84. Xu, H.; Xu, Z.; Liu, P. Estimation of Nonpoint Source Pollutant Loads and Optimization of the Best Management Practices (BMPs) in the Zhangweinan River Basin. *Environ. Sci.* **2013**, *34*, 882–891. (In Chinese) [CrossRef]

85. Kang, M.S.; Park, S.W.; Lee, J.J.; Yoo, K.H. Applying SWAT for TMDL programs to a small watershed containing rice paddy fields. *Agric. Water Manag.* **2006**, *79*, 72–92. [CrossRef]

86. Lü, Y.; Ma, Z.; Zhang, L.; Fu, B.; Gao, G. Redlines for the greening of China. *Environ. Sci. Policy* **2013**, *33*, 346–353. [CrossRef]

87. Xu, X.; Tan, Y.; Yang, G.; Barnett, J. China's ambitious ecological red lines. *Land Use Policy* **2018**, *79*, 447–451. [CrossRef]

88. Diyabalanage, S.; Samarakoon, K.K.; Adikari, S.B.; Hewawasam, T. Impact of soil and water conservation measures on soil erosion rate and sediment yields in a tropical watershed in the Central Highlands of Sri Lanka. *Appl. Geogr.* **2017**, *79*, 103–114. [CrossRef]

89. Wenger, A.S.; Atkinson, S.; Santini, T.; Falinski, K.; Hutley, N.; Albert, S.; Horning, N.; Watson, J.E.M.; Mumby, P.J.; Jupiter, S.D. Predicting the impact of logging activities on soil erosion and water quality in steep, forested tropical islands. *Environ. Res. Lett.* **2018**, *13*, 044035. [CrossRef]

90. Gonzalez, S.O.; Almeida, C.A.; Calderon, M.; Mallea, M.A.; Gonzalez, P. Assessment of the water self-purification capacity on a river affected by organic pollution: Application of chemometrics in spatial and temporal variations. *Environ. Sci. Pollut. Res.* **2014**, *21*, 10583–10593. [CrossRef]